

Intrinsic exciton-exciton coupling in GaN-based quantum dots: Application to solid-state quantum computing

S. De Rinaldis,^{1,2} I. D'Amico,^{1,3} E. Biolatti,^{1,4} R. Rinaldi,^{1,2} R. Cingolani,^{1,2} and F. Rossi^{1,3,4}

¹*Istituto Nazionale per la Fisica della Materia (INFN)*

²*National Nanotechnology Laboratory (NNL), Università di Lecce, via per Arnesano, Lecce, Italy*

³*Institute for Scientific Interchange (ISI), Villa Gualino, Viale Settimio Severo 65, I-10133 Torino, Italy*

⁴*Dipartimento di Fisica, Politecnico di Torino, Corso Duca degli Abruzzi 24, I-10129 Torino, Italy*

(Received 24 August 2001; revised manuscript received 5 November 2001; published 8 February 2002)

In this Rapid Communication we propose to use GaN-based quantum dots as building blocks for solid-state quantum-computing devices. The existence of a strong built-in electric field induced by the spontaneous polarization and by the piezoelectricity is exploited to generate entangled few-exciton states in coupled quantum dots without resorting to external fields. More specifically, we shall show how the built-in field induces intrinsic exciton-exciton coupling, which can be used to realize basic quantum information processing on a sub-picosecond time scale.

DOI: 10.1103/PhysRevB.65.081309

PACS number(s): 73.21.La, 78.47.+p, 03.67.-a

The introduction of quasi-zero-dimensional (0D) systems, called semiconductor quantum dots (QDs), represented a real scientific and technological “revolution” in the field of semiconductor nanostructures.¹ Compared to systems of higher dimensionality—like quantum wells and wires—they have a discrete, i.e., atomiclike, energy spectrum and, more important, they exhibit genuine few-carrier effects. Apart from their relevance in terms of basic physics, these semiconductor nanostructures have attracted general attention because of their potential technological applications: these include coherent light sources,² charge-storage devices,³ fluorescent biological markers,⁴ and quantum information processing devices.⁵

The quantized, atomiclike, energy structure of QDs allows for a rich optical spectrum and for a weak interaction of the QD system with environmental degrees of freedom (like phonons, plasmons, etc.), i.e., for an almost decoherence-free quantum evolution of the carrier subsystem.⁶ Moreover, their reduced spatial extension—up to few nanometers—leads to an increase of two-body interactions among carriers and to stronger Coulomb-correlation effects.⁷

As recently proposed in Ref. 8, a proper combination of these two unique features may allow us to realize *fully optical quantum gates*. In this scheme, interband optical excitations are used as *computational degrees of freedom*: the basis states $|1\rangle$ and $|0\rangle$ of the quantum bit (*qubit*) correspond, respectively, to the presence or absence of ground-state excitons in a QD array. Single- and two-qubit operations are driven by ultrafast sequences of multicolor laser pulses, and two-qubit interactions are controlled by exciton-exciton dipole coupling.⁸

However, one of the major technological problems in implementing the solid-state quantum gate proposed in Ref. 8 is the need of an external electric field to drive two-qubit conditional operations. Indeed, from the technological point of view, this requires the presence of electrical contacts which limit the time response of the system and strongly complicate the physical interconnection of the device. The ideal scheme would thus be a QD structure with built-in electric fields. GaN-based quantum dots seem to match quite

well these requirements,⁹ as they are known to exhibit strong built-in polarization and piezoelectric field (of the order of MV/cm).

To overcome this limitation, in this Rapid Communication we propose an all-optical quantum gate based on a GaN QD molecule. The central idea is to properly tailor the internal field such to induce built-in exciton dipoles. This will result in an intrinsic exciton-exciton coupling, i.e., without the need of additional external fields. We shall show that the biexcitonic shift due to such dipole-dipole interaction is of the order of a few meV, thus allowing for subpicosecond quantum-state manipulations via ultrafast laser-pulse sequences.

As already mentioned, one of the most interesting features of GaN heterostructures is the strong built-in electric field: this is induced both by the spontaneous polarization and by the piezoelectric field. Contrary to GaN quantum wells—where the major role is played by the spontaneous polarization charge accumulated at the GaN/AlGaIn interfaces while strain-induced piezoelectric fields have a minor importance¹⁰—in GaN QDs piezoelectric effects become relevant because of the noncentral symmetry of the wurzite structure. Moreover, since the dimensions of the GaN and AlN unit cell differ slightly from those of an ideal hexagonal crystal, a spontaneous electrostatic polarization is present as well.⁹ As shown in Ref. 9, the strain-induced piezoelectric potential and the spontaneous-polarization contribution are of similar magnitude and equal sign, both oriented along the growth direction. The magnitude of the intrinsic electric field along the growth direction is almost the same inside and outside the dot, but it is opposite in sign.¹¹

The internal field in GaN QDs can be tailored varying the size of the dot: the total electric field inside the dot is¹⁰

$$F_d = \frac{L_{br}(P_{tot}^{br} - P_{tot}^d)}{\epsilon_0(L_d \epsilon_{br} + L_{br} \epsilon_d)}, \quad (1)$$

where $\epsilon_{br,d}$ is the relative dielectric constant of the barrier and of the quantum dot, $P_{tot}^{br,d}$ is the total polarization, and $L_{br,d}$ is the width of the barrier and the height of the dot. The

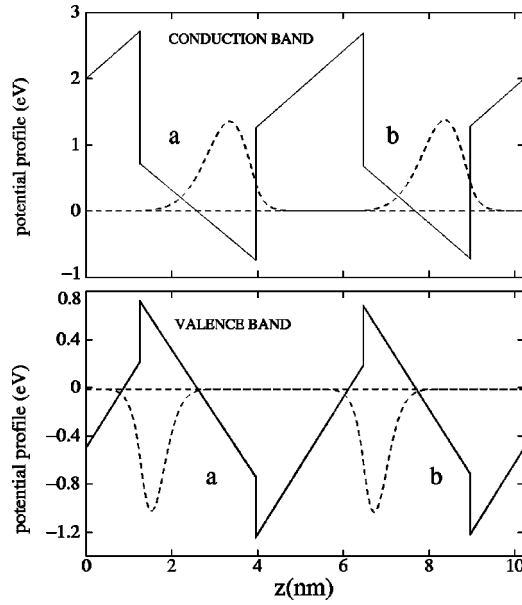


FIG. 1. Effects of the intrinsic electric field in a GaN-based QD structure: schematic representation of the square-well potential profile for electrons and holes along the growth direction modified by the internal field (solid lines) and single-particle spatial charge distributions for electrons (e_a and e_b) and holes (h_a and h_b) (dashed curves).

value of the field in the barrier F_{br} is obtained by interchanging the indices br and d . Equation (1) is derived for an alternating sequence of quantum wells and barriers, but we can consider it as a good approximation for our case, since we consider an alternating sequence of QDs and barriers in the growth (z) direction. We stress that Eq. (1) provides fields in very good agreement with the experimental findings of Ref. 9. This relatively simple model neglects the in-plane shape of the QD: we will consider the lateral shape of the dot as to be simply responsible for the relatively strong in-plane carrier confinement,⁹ which can be well described in terms of a 2D parabolic potential.

The polarization is the sum of the piezoelectric charge P_{piezo} induced by the lattice mismatch (ms) and by the thermal strain (ts) ($P_{piezo}^{br/d} = P_{ms}^{br/d} + P_{ts}^{br/d}$) and the spontaneous polarizability $P_{sp}^{br/d}$ of the GaN/AlN interface: $P_{tot}^{br/d} = P_{piezo}^{br/d} + P_{sp}^{br/d}$. Such a built-in electric field induces electron-hole dipoles in each QD. This, in turn, will generate an interdot dipole-dipole coupling. For the case of two stacked QDs a and b along the growth (z) direction (see Fig. 1) for which $\mathbf{p}_i \parallel \hat{z}$, \mathbf{p}_i the dipole moment of the i dot, we get

$$\Delta\mathcal{E} = -2(p_a p_b / Z^3), \quad (2)$$

where Z is the distance between the two dipoles.

The general scheme of our two-qubit quantum gate consists of two stacked dots of slightly different size.¹² For the sake of clarity, here we discuss the case of two coupled dots with identical bases, stacked along the growth axis, and having a height of 2.5 and 2.7 nm, respectively. Analogous results would be obtained by two dots of same height and different base radius. The resulting difference in the

potential-well width w_d of each QD ($\delta w_d \approx 0.2$ nm) allows us to shift the excitonic transitions (see below). Moreover, the barrier width w_{br} is chosen such to prevent single-particle tunneling but to allow at the same time for significant dipole-dipole Coulomb coupling. We have evaluated the internal electric field according to Eq. (1), where $P_{ms}^{br/d} = -2(e_{33}C_{13}/C_{33} - e_{31})\sigma_{\parallel}^{br/d}$ (all the material parameters can be found in Ref. 10, except for the lattice in-plane mismatch σ_{\parallel}^{br} that is here 2.48%), $P_{ts}^d = -3.2 \times 10^{-4}$ C/m², $P_{ts}^{br} = 0$ C/m², $P_{sp}^{br} = -0.081$ C/m², and finally $P_{sp}^d = -0.029$ C/m². The values used for σ_{\parallel}^{br} and P_{sp}^{br} take into account the increased percentage of Al ($x = 1$) in the barrier with respect to Ref. 10 ($x = 0.15$).

Given these parameters, we have calculated the electric field for a 2.7 nm height dot and a 2.5 nm barrier obtaining fields of $F_d = 5.8$ MV/cm in the barrier and $F_d = 5.4$ MV/cm in the dot. Starting from these results, and in order to take into account the slightly different size of the two coupled QDs, we used in our calculations the fields $F_d = 5.6$ MV/cm and $F_d = 5.4$ MV/cm for the two dots and $F_{br} = 5.7$ MV/cm for the barrier; this choice allows for a potential profile that is periodic over the two-dot cell. The electric field strongly modifies the conduction-band and valence-band edges along the growth directions (see Fig. 1); this causes the spatial separation of the carrier states and the creation of intrinsic dipoles as it can be seen in Fig. 1. Here, the internal field shifts in opposite directions the electron and the hole charges: electrons are forced to move towards the top of the dot (right) and holes are driven towards its bottom (left). So, if we consider two dots (a and b) along the growth direction and with one exciton each, we are left with two aligned dipoles which are both pointing in the same direction. As recalled before, this results in a negative dipole-dipole coupling term [see Eq. (2)]. The energy shift $\Delta\mathcal{E}$ is opposite and its absolute value is doubled with respect to the configuration of Ref. 8, in which the two dipoles are still parallel but laying side by side.

Let us now discuss the optical response of our *semiconductor macromolecule* ($a + b$) in Fig. 1. Our calculations are based on the fully three-dimensional approach of Ref. 8. The excitonic absorption spectrum in the presence of the intrinsic field is shown in Fig. 2 (solid curve). The two lowest optical transitions correspond to the formation of direct ground-state excitons in dot a and b , respectively. Due to the strong built-in electric field in such heterostructures, it is known that the excitonic transitions energies are redshifted and, as it can be seen in Fig. 2, the interband emission is fractions of eV below the GaN bulk band-gap energy (3.5 eV) (see also Fig. 1). It is worth noticing that the difference in the ground-state excitonic transitions of the two dots is one order of magnitude bigger than the one employed in Ref. 8, and this is due to the presence of the strong intrinsic electric field in the growth direction. Moreover, the two ground-state transitions have different amplitudes, due to the nonsymmetric structure we are considering: indeed, the two dots have different heights along the growth direction, which implies that the internal electric field experienced by the carriers in each dot is not the same. As a result the oscillator strength—i.e.,

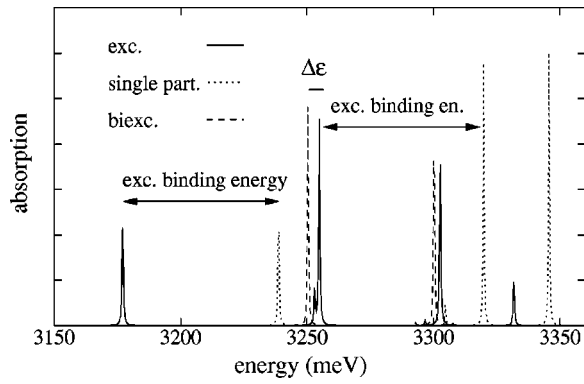


FIG. 2. Optical response of the GaN-based QD macromolecule of Fig. 1. Excitonic (solid curve) and biexcitonic absorption (dashed curve). The latter has been computed assuming as initial state an exciton in dot a and the laser pulses are supposed to have the same circular polarization. The single-particle spectrum is also reported (dotted curve) as well as the corresponding exciton binding energy.

the overlap of electron and hole single-particle wave functions—changes according to the specific dot. The peaks which occur at higher energies correspond to optical transitions involving excited states of the in-plane parabolic potential in each QD.

We stress that, since the electric field is in the growth direction, the in-plane 2D confinement potentials for electrons and holes exhibit the same symmetry axis. It follows that, due to parity arguments, only a few interband optical transitions are allowed, which makes the interpretation as well as the energy-selective addressing of specific lines in the spectrum much easier. This is a distinguished advantage of the proposed GaN-based scheme, compared to the implementation in Ref. 8, where the presence of the in-plane field breaks all interband selection rules related to the 2D cylindrical symmetry of single-particle wave functions. This feature may be of crucial importance when considering energy-selective addressing schemes, since it allows to employ shorter light pulses, i.e., pulses with a larger spectral width.

Let us now discuss the biexcitonic spectrum (dashed curve in Fig. 2); it describes the generation of a second electron-hole pair in the presence of a previously created exciton ($1 \rightarrow 2$ optical transitions). The crucial feature in Fig. 2 is the magnitude of the “biexcitonic shift,”¹¹ i.e., the energy difference between the excitonic and the biexcitonic transition (see solid and dashed curves). For the QD structure under investigation we get an energy splitting of 4.4 meV, which is comparable to the one in Ref. 8 and can still be resolved by sub-picosecond optical excitations.

In order to test the viability of the proposed semiconductor-based quantum hardware (in the framework of the quantum-computing scheme proposed in Ref. 8), we have performed a few simulated experiments of basic quantum information/computation (QIC) processing. Our time-dependent simulations are based on the realistic state-of-the-art multi-QD structure of Fig. 1 for which $\mathcal{E}_a = 3.177$ eV, $\mathcal{E}_b = 3.255$ eV, and $\Delta\mathcal{E} = -4.4$ meV (see Fig. 2). The simulations are based on a numerical solution of the Liouville–von Neumann equation describing the exact quantum-

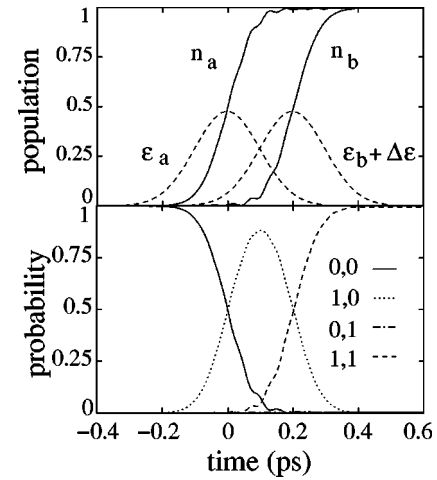


FIG. 3. Time-dependent simulation of a two-qubit operation realizing the first prescription ($|1,0\rangle \rightarrow |1,1\rangle$) of a CNOT logic quantum gate in the coupled QD structure $a+b$ of Fig. 1 (see text). Exciton populations n_a and n_b (upper panel) and diagonal density-matrix elements (lower panel) as a function of time. The laser-pulse sequence is also sketched (dashed curve in the upper panel). We stress that the initial π pulse is only used to transform the original ground state $|0,0\rangle$ to the initial state $|1,0\rangle$ of the CNOT.

mechanical evolution of the many-exciton system within our computational subspace in the presence of environment-induced decoherence processes. The latter are accounted for within our simulation in terms of a standard $T_1 T_2$ model. More specifically, interband recombination is described in terms of a $T_1 = 1$ ns while exciton-phonon dephasing is accounted for by a time $T_2 = 50$ ps. Due to the strong electron-hole charge separation, exciton-phonon coupling in GaN-based materials is expected to be somewhat stronger than in GaAs-based structures, for which dephasing times up to 600 ps have been recently measured.¹³ Therefore, the T_2 value used in our simulated experiments seems to be a safe underestimation of the real value, which is still experimentally unknown.

Figure 3 shows a simulated sequence of two-qubit operations driven by a two-color laser-pulse sequence (dashed curve in the upper panel). This realizes the well-known conditional NOT (CNOT) quantum gate: the state of the second quantum dot is changed if and only if the first dot is in the state $|1\rangle$. Indeed, the multicolor laser-pulse train is able to perform first a π rotation of the qubit a ($|0\rangle_a \rightarrow |1\rangle_a$); then, the second pulse is tuned to the frequency $\mathcal{E}_b + \Delta\mathcal{E}$, thus performing a π rotation of the qubit b ($|0\rangle_b \rightarrow |1\rangle_b$), since this corresponds to its renormalized transition energy when the neighbor qubit a is in state $|1\rangle_a$. The scenario described so far is confirmed by the time evolution of the exciton occupation numbers n_a and n_b (upper panel) as well as of the diagonal elements of the density matrix in our four-dimensional computational basis (lower panel). The operation is performed in a subpicosecond time scale; in particular, the time delay between the pulses is only $\delta t = 0.2$ ps.

Let us now come to the ultrafast generation of entangled states shown in Fig. 4. As for the CNOT gate simulated in Fig. 3, initially, the system is in the state $|0,0\rangle \equiv |0\rangle_a$

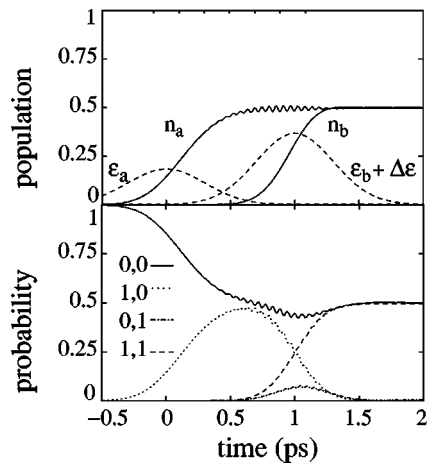


FIG. 4. Time-dependent simulation of a CNOT quantum gate transforming the factorized state $|0,0\rangle + |1,0\rangle$ into a maximally entangled state $|0,0\rangle + |1,1\rangle$ for the coupled QD structure $a + b$ in Fig. 1 (see text). Exciton populations n_a and n_b (upper panel) and diagonal density-matrix elements (lower panel) as a function of time. The laser-pulse sequence is also sketched (dashed curve in the upper panel). We stress that the initial $\pi/2$ pulse is only used to transform the original ground state $|0,0\rangle$ to the initial state $|0,0\rangle + |1,0\rangle$ of the CNOT.

$\otimes |0\rangle_b$. The first laser pulse (at $t=0$) is now tailored in such a way to induce a $\pi/2$ rotation of the qubit a : $|0,0\rangle \rightarrow (|0,0\rangle + |1,0\rangle)/\sqrt{2}$. At time $t=0.4$ ps a second pulse induces a conditional π rotation of the qubit b : $|0,0\rangle + |1,0\rangle \rightarrow |0,0\rangle + |1,1\rangle$. We stress that the conditional operation simulated in Fig. 4 plays a central role in any quantum information processing. Indeed, it shows how it is possible to transform a *factorized* state $[(|0\rangle + |1\rangle) \otimes |0\rangle]$ into an *entangled* state.

In summary, we have proposed a scheme for implementing an *all-optical* QIC processing, which exploits the char-

acteristic built-in electric fields typical of GaN-based semiconductor nanostructures. Our analysis has shown that energy-selected optical transitions in realistic state-of-the-art GaN QD structures are good candidates for quantum-information encoding and manipulation. In particular, the subpicosecond time scale of ultrafast laser spectroscopy allows for a relatively large number of elementary operations within the exciton decoherence time. Indeed, the experiments simulated above clearly show that the energy scale of the exciton-exciton coupling in our QD molecule (see Fig. 2) is compatible with the subpicosecond operation time scale (see Figs. 3 and 4).

At this point, it is worth summarizing the various advantages given by the intrinsic built-in electric field of nitride-based QDs. First of all, one does not need to apply external fields to the QD structure. This allows for an easier implementation of the all-optical QIC processing proposed in Ref. 8. Second, since the internal field is oriented along the growth direction, the single-particle angular momentum in each allowed interband transition is conserved and the usual interband selection rules are now restored. This implies simpler spectra, which in turn makes individual absorption lines easier to identify and to energetically address experimentally. Last but not least, due to the built-in electric field, the ground-state excitonic transitions employed for quantum information processing are significantly separated with an energy difference of about one order of magnitude larger with respect to the scheme in Ref. 8.

The open question is still the control and characterization of GaN QDs, whose technology is recognized to be far less mature than the GaAs-based one. However, a lot of work is in progress both on the theoretical and on the experimental side, and such purely technological gap, we believe, will be strongly reduced in the next future.

This work has been supported in part by the European Commission through the Research Project *SQID* within the *Future and Emerging Technologies (FET)* program.

¹See, e.g., L. Jacak, P. Hawrylak, A. Wojs, *Quantum Dots* (Springer, Berlin, 1998); D. Bimberg *et al.*, *Quantum Dot Heterostructures* (Wiley, Chichester, 1998).

²See, e.g., H. Saito *et al.*, *Appl. Phys. Lett.* **78**, 267 (2001).

³See, e.g., T. Lundström *et al.*, *Science* **286**, 2312 (1999).

⁴See, e.g., M. Jr. Bruchez *et al.*, *Science* **281**, 2013 (1998).

⁵See, e.g., D. Loss and D.P. DiVincenzo, *Phys. Rev. A* **57**, 120 (1998); M. Sherwin *et al.*, *ibid.* **60**, 3508 (1999).

⁶See, e.g., P. Zanardi and F. Rossi, *Phys. Rev. Lett.* **81**, 4752 (1998).

⁷See, e.g., R. Rinaldi *et al.*, *Phys. Rev. B* **62**, 1592 (2000); I. D'Amico and F. Rossi, *Appl. Phys. Lett.* **79**, 1676 (2001).

⁸E. Biolatti, R.C. Iotti, P. Zanardi, and F. Rossi, *Phys. Rev. Lett.* **85**, 5647 (2000).

⁹R.D. Andreev and E.O. O'Reilly, *Phys. Rev. B* **62**, 15 851 (2000); F. Widmann *et al.*, *ibid.* **58**, R15 989 (1998).

¹⁰R. Cingolani *et al.*, *Phys. Rev. B* **61**, 2711 (2000).

¹¹One of the advantages of having a strong intrinsic electric field, instead of an external one as proposed in Ref. 8, is that carriers remain trapped into the dot. In the presence of an external field, in fact, carriers may escape from the dot, due to the finite height of the lateral confinement potential.

¹²Two dots systems grown epitaxially can be tailored in such a way that the seeding dot is smaller than the topmost dot, due to the overlap of the strain fields, or the two dots having identical base diameter but slightly different height, thanks to the control in the deposition rate and III-V ratio. In both cases, the confinement potential of the two dots is engineered such to control the splitting of the respective ground-state energy levels, thus allowing for selective optical excitation of one of the two dots by ultrafast laser pulses.

¹³See, e.g., *Proceedings of the 7th International Conference on Optics and Excitons in Confined Systems (OECS7), Montpellier, France, 2001* [Phys. Status Solidi (to be published)].